International Journal of Innovation in
Mechanical Engineering and Advanced Materials
Journal homepage: publikasi.mercubuana.ac.id/index.php/ijimeam
Vol. 8 (No. 3), 2026, Art. No. 39654, pp. 191-205
DOI: 10.22441/ijimeam.v8i3.39654

Article

Comparative Assessment of Industrial Heat Pump Configurations for Spray Drying Dairy Manufacturing

Imron Afandi [1], A. Hakim Ermanu [1,*], Sulianto [1], Noufal Haneef [2], and Alrafly Rizky Putra Henryansyah [3]

[1]Master Program of Renewable Engineering, University of Muhammadiyah Malang, Tegalgondo, Malang 61450, Indonesia
[2]Department of Electrical Engineering, University of Muhammadiyah Malang, Tegalgondo, Malang 61450, Indonesia
[3]Department of Mechanical Engineering, State University of Surabaya, Ketintang Campus, Surabaya 60213, Indonesia
*Corresponding Author: ermanu@umm.ac.id (AHE)

Abstract

Heat pumps (HPs) are a key route to industrial decarbonization through electrification, but selecting a configuration requires more than maximizing thermodynamic performance: a highly efficient system may still be unable to supply the steam pressure and temperature that a process needs. Few studies evaluate HP configurations by combining thermodynamic performance with process delivery capability. This study compares four configurations of increasing complexity with a boiler–chiller baseline: (C1) boiler feedwater preheating, (C2) a simultaneous heating and cooling HP, (C3) a two-stage cascade high-temperature HP (HTHP), and (C4) a cascade HTHP with mechanical vapor recompression (MVR). The case is a dairy spray-drying plant that requires 12 barg steam (4 t/h) and 250 TR of cooling. Energy and exergy analyses used IAPWS-IF97 properties and the Gouy–Stodola formulation. Each COP was tested against its Lorenz limit and replaced by a cycle-based value where inadmissible, and C3 was modelled independently of C4. At the design point, exergy efficiency rose from 25.5% (baseline) to 27.4% (C1), 29.1% (C2), 34.5% (C3) and 42.2% (C4). Only C4 delivered 12 barg steam; C3 supplied saturated steam at 4 barg (152 °C). The vendor quoted COP of C2 (5.3) exceeded its Lorenz limit (5.12) and was replaced by a cycle-calculated value of 2.56. Operational CO_2 emissions of C3 and C4 exceed those of the baseline when the grid emission factor is above about 0.30 t CO_2/MWh (0.88 t CO_2/MWh was adopted). Delivery-envelope compliance and exergy efficiency are independent criteria: compliance is decided by the final steam pressure, whereas the exergy efficiency of C3 ranged from 31.6% to 60.0% across the sensitivity grid without changing its 4 barg limit. The proposed framework checks delivery-envelope compliance first and Lorenz-consistent thermodynamic performance second, allowing unsuitable configurations to be excluded before detailed techno-economic design.

Article Info:
Received: 7 August 2026
Revised: 21 October 2026
Accepted: 10 November 2026
Available online: 23 November 2026

Keywords:
cascade heat pump; Lorenz-limit validation; industrial heat pump; mechanical vapor recompression; spray-drying dairy manufacturing

© 2026 The Author(s). Published by Universitas Mercu Buana (Indonesia). This is an open-access article, distributed under *CC BY-SA* License.

1. Introduction

Process heat accounts for about two-thirds of global industrial energy use, and in the less energy-intensive sectors (food and beverages, textiles, light manufacturing) some 75% of the heat requirement lies below 200 °C [1]. In the food and beverage sector, 54.0% of process heat is required below 100 °C and 86.5% below 200 °C [2], largely within the reach of commercial industrial heat pumps (HPs) [3], [4]. Dairy spray drying sits at the demanding end of this window: pressurized steam is needed for evaporation while chilled water is needed simultaneously for product cooling and air-conditioning [5], [6]. When the two duties are met by a boiler and a separate chiller, heat is rejected to ambient while fuel is burned to raise steam, an avoidable irreversibility that industrial HPs can reduce [7], [8]. With HPs projected to supply about 30% of low- to medium-temperature heat in light industry by 2050 under a net-zero trajectory [9], selecting an HP configuration is an immediate engineering problem.

How to cite:

I. Afandi, A. H. Ermanu, Sulianto and N. Haneef, and A. R. P. Henryansyah "Comparative assessment of industrial heat pump configurations for spray drying dairy manufacturing," *Int. J. Innov. Mech. Eng. Adv. Mater.*, vol. 8, no. 3, pp. 191-205, 2026

Industrial HP technologies range from feedwater preheaters to cascade high-temperature heat pumps (HTHPs) with mechanical vapor recompression (MVR). Their suitability depends on two independent factors: whether they can deliver the required temperature and pressure, and how efficiently they operate. Feedwater preheaters achieve a high COP through a small lift but still rely on the boiler; simultaneous heating and cooling heat pumps (SHC-HPs) can replace chillers while supplying hot water but cannot produce pressurized steam; only cascade HTHPs, especially with MVR, can provide steam at 12 barg [10]; an experimental HTHP prototype delivered steam-range heat at about 150 °C [11]. High efficiency alone therefore does not guarantee that a configuration meets the process requirement.

Several studies frame the present work. Bellos et al. [12] show that small lifts give a high COP and that feasibility falls quickly as delivery temperature rises, confining low-lift options to feedwater preheating. Ahrens et al. [8] show that combined heating and cooling outperforms separate systems when demands coincide, but for hot-water duties only. Adamson et al. [13] report that commercial HTHPs have consolidated at 100–160 °C supply temperature. Hu et al. [14] and Wu et al. [15] report cascade exergy efficiencies of about 60–70% at large lift, but for heat pumps alone. Hu et al. [16] extend the exergy approach to an advanced exergy and exergoeconomic analysis of a cascade HTHP recovering low-temperature waste heat. Ma et al. [10] evaluate a HTHP steam system on energy, exergy, economic and environmental criteria, and Ramirez et al. [11] demonstrate experimentally the delivery of steam-range heat at 148.5 °C, below the 191 °C of a 12 barg header. Dong and Wang [17] give multi-criteria guidance on when a cascade is justified. For dairy plants, Walmsley et al. [5] report a 51.5% reduction in thermal energy use for milk powder production by combining MVR evaporation with dryer-exhaust heat recovery, and Schlosser et al. [6] determine the economic break-even of HTHP integration for milk spray drying.

These studies show that exergy efficiency and delivery pressure are governed by different design variables. Among the studies reviewed, none evaluates both for the same case on one property basis, and none tests vendor-quoted COP values against a thermodynamic limit before the comparison (Table 1). A configuration can therefore rank first on efficiency and still be unable to supply the required steam header.

The contribution of this study is threefold. First, compliance with the required steam pressure and temperature is applied as a pass/fail gate before configurations are ranked, in contrast to multi-criteria approaches that combine efficiency and other indicators in a single score [6], [17]. Second, design COP values are tested against the Lorenz limit of the actual source and sink temperature profiles, and a cycle calculation, not a correction factor, provides the replacement value where a design value is inadmissible. Third, a boiler–chiller baseline and four configurations, (C1) feedwater preheating, (C2) an SHC-HP, (C3) a two-stage cascade HTHP and (C4) a cascade HTHP with MVR to 12 barg, are evaluated for a dairy spray-drying plant in Mojokerto, Indonesia, on one property, exergy and operating basis. The framework is a procedure rather than a new thermodynamic model, the numerical results apply to the case studied, and economic aspects are excluded because they are site-specific.

The objectives are as follows. Scientific objectives: (S1) to compare the first-law and second-law performance of a boiler–chiller baseline and four HP configurations (C1–C4) on one stated operating basis; (S2) to test each design COP against a thermodynamically consistent limit and to establish a cycle-based COP where the design value is not admissible; (S3) to determine whether ranking by exergy efficiency and ranking by delivery-envelope compliance agree. Practical objectives: (P1) to identify which configurations can supply 12 barg

Table 1. Research gap matrix: analytical dimensions addressed by principal reference studies compared with this study.

Reference	Multi-Config Comparison	Exergy Analysis	Lorenz Validation	Pressurized Steam (MVR)	Delivery-Envelope Criterion
[8]	–	–	–	–	–
[14]	–	✓	–	–	–
[15]	✓ (3 types)	✓	–	–	–
[5]	–	–	–	✓	–
[6]	✓ (MCDA)	–	–	–	–
[12]	–	–	–	–	✓
This Study (C1–C4)	✓ (4 configs)	✓	✓ (Lorenz limit + cycle COP)	✓	✓

(191 °C) steam and 6 °C chilled water without auxiliary equipment; (P2) to provide a two-step screening framework that a plant can apply before techno-economic assessment.

2. Methods

2.1. Study object, data sources, and system boundaries

The case is the utility system of a dairy spray-drying facility in Mojokerto, East Java: a natural-gas-fired boiler rated at 4 t/h of saturated steam at 12 barg (191 °C) and a 250 TR (879 kW) R134a screw chiller supplying chilled water at 6/12 °C, operating 24 h/day and 320 days/year (7,680 h/yr). The recorded gas consumption of 400,000 m^3/yr (4.2 GWh/yr at a lower heating value, LHV, of 10.5 kWh/m^3; 760 t CO_2/yr) and chiller-system electricity of 3.87 GWh/yr refer only to this boiler and chiller; the gas record corresponds to a boiler load factor of 0.158 (Section 2.8). The boundary is the utility side: heat pump(s), boiler, chiller and heat exchangers up to the point of distribution. Pumps, fans and auxiliaries are excluded from the electricity balance, and photovoltaics, storage and capital cost are outside the scope.

2.2. Analytical workflow

The same seven stages were applied to the baseline and C1–C4: (1) plant data (Table 4); (2) baseline duties verified against the rating and metered gas (Section 2.8); (3) configuration design (Table 2) for the same 12 barg steam and 6 °C chilled-water duty; (4) energy balances, Equations (1)–(6); (5) COP validation, Equations (14)–(16), with cycle-based replacement (Section 2.6); (6) exergy analysis, Equations (7)–(13), at T0 = 298.15 K; and (7) the selection framework (Section 2.7). Stages 4–6 were repeated for the sensitivity cases.

Properties were evaluated with IAPWS-IF97 [18] for water and steam and with CoolProp 8.0.0 [19] for R-744, R-134a, R-1233zd(E) and HFO-1336mzz(Z) (equations of state [20]–[23]). The calculation was implemented in a spreadsheet and reproduced independently in a Python script calling CoolProp 8.0.0; the two agreed to a relative difference of 10−14 on 140 compared outputs, which verifies the arithmetic but is not a validation against measurements. The script generated the state points of every stage (Supplementary Tables S2–S6). No dynamic simulation was performed, so part-load behaviour is outside the scope. All inputs needed to reproduce the results are given in Tables 2 and 4.

2.3. Definition of the four heat pump configurations

Four configurations of increasing complexity are evaluated on the same boundary (Figure 1, Table 2). C1 – Preheater HP: a single-stage water-to-water HP installed in parallel with the boiler produces 6 °C chilled water, taking over the part of the chiller duty equal to its evaporator duty, and preheats boiler feedwater from 25 °C to 70–80 °C; the boiler remains the sole steam source at reduced load. C2 – SHC-HP: a single HP delivers a 70–85 °C hot-water

Table 2. Definition and design-point attributes of the four evaluated heat pump configurations.

Attribute	C1-Preheater	C2-SHC-HP	C3-Cascade HTHP	C4-Cascade HTHP+MVR
No. of thermodynamic stages	1	1	2	3
Delivered form	Hot water (feedwater preheat only)	Hot water 70–85 °C + CHW 6 °C	Saturated steam 4 barg / 152 °C + CHW 6 °C	Pressurized steam 12 barg / 191 °C + CHW 6 °C
Meets 12 barg header directly	No (boiler retained)	No (boiler retained)	No (limited to ≤4 barg)	Yes
Condenser/steam output at design point (kW)	232.4	1,100	2,423.1 (4 barg, 82.5% of duty)	2,688.9 (HP steam generator, 4 barg); 2,979.7 (delivered steam, 12 barg)
Compressor power at design point (kW)	67.0	429.2	1,814.1 (891.0 + 923.1)	2,303.9 (988.7 + 1,024.4 + 290.8 MVR)
Design (vendor) COP	5.1	5.3	3.5 (S1) / 2.7 (S2)	3.5 / 2.7 (S1/S2); MVR η_is 70% (S3)
Cycle COP (this study)	3.47	2.56	1.68 (S1) / 2.62 (S2)	1.68 / 2.62 (S1/S2); MVR η_is 70% (S3)

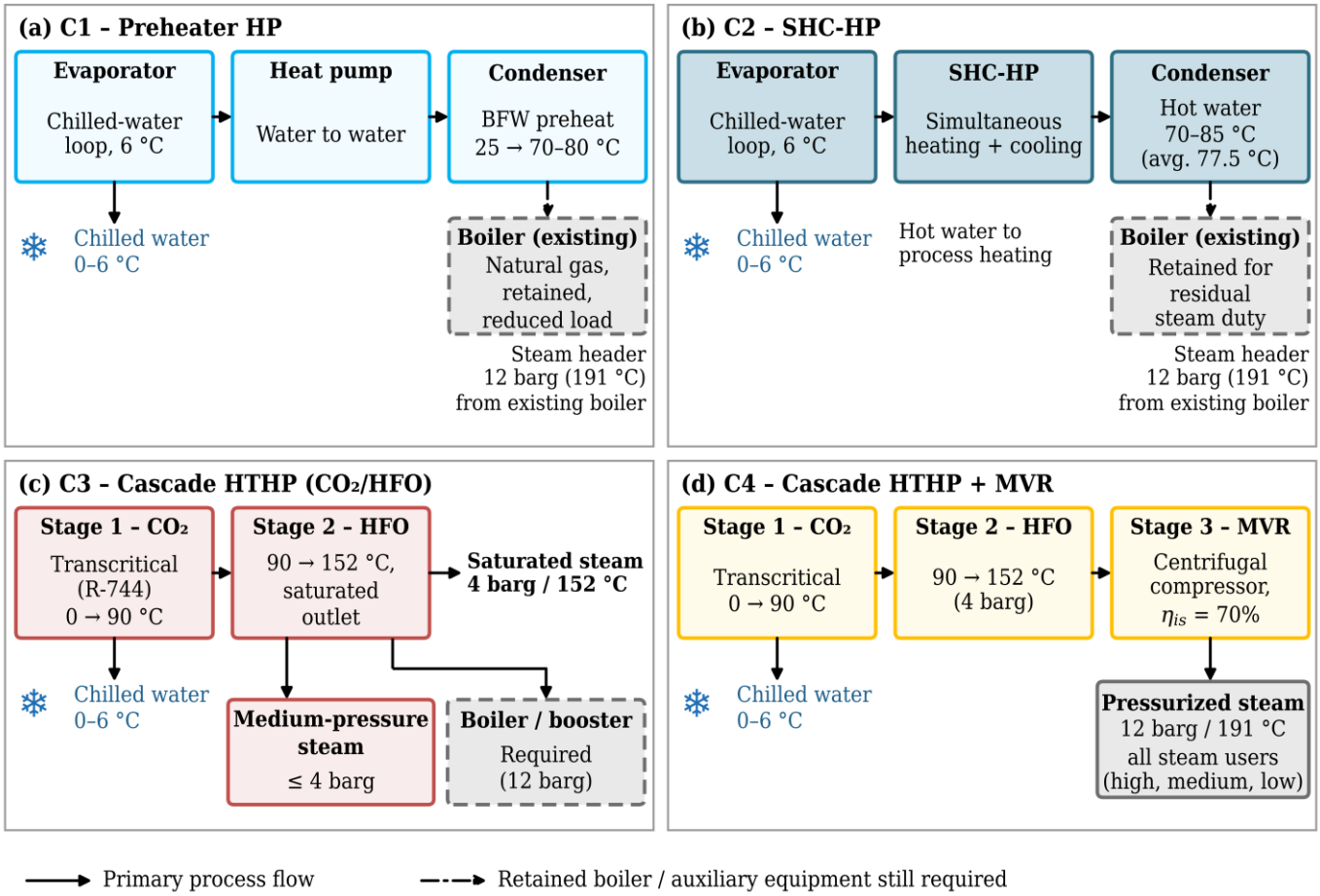


Figure 1. Baseline utility system and the four heat pump configurations: (a) C1 – Preheater HP (boiler retained); (b) C2 – SHC-HP (hot water and part of the chilled water); (c) C3 – Cascade HTHP (CO_2/HFO), saturated steam at 4 barg, boiler retained for the 12 barg header; (d) C4 – Cascade HTHP+MVR, steam boosted to the 12 barg/191 °C header without boiler gas.

loop (mean condenser temperature 77.5 °C) and 6 °C chilled water, displacing part of the chiller duty; the boiler remains in service for all steam duties.

C3 – Cascade HTHP without pressure boosting: Stage 1 (transcritical CO_2, R-744) evaporates at 0 °C (34.9 bar), supplying chilled water, and cools the supercritical gas to 90 °C; Stage 2 (HFO-1336mzz(Z)) evaporates at 85 °C (4.89 bar) and condenses at 157 °C (22.5 bar), generating saturated steam at 4 barg (152 °C). In the independent model (Section 3.4.2), 82.5% of the steam duty (3,300 kg/h; 2,423.1 kW) is raised at 4 barg and 17.5% by the retained boiler at 12 barg; the share f_4 = 0.825 is an assumption varied between 0.7 and 1.0 (Table S1). The compressor powers (Table 2) follow from the cycle COPs of 1.68 and 2.62 (Section 3.3); the design COPs of 3.5 and 2.7 are used only in the sensitivity analysis. Because 4 barg is below the header pressure, C3 can directly serve only medium-pressure users.

C4 – Cascade HTHP+MVR: a centrifugal MVR (isentropic efficiency 0.70) compresses the 4 barg steam of Stage 2 to the 12 barg (191 °C) header, followed by a feedwater desuperheater. Because the HP steam generator supplies the entire steam duty (2,688.9 kW), the compressor powers of Stages 1 and 2 are 988.7 kW and 1,024.4 kW, and the MVR shaft power is 290.8 kW (Section 2.4). C4 fully electrifies the steam duty and eliminates boiler gas; the chilled water not supplied by Stage 1 remains with the existing chiller.

2.4. Energy balance (first law)

The first law is applied to each heat pump stage in steady flow, with negligible kinetic and potential energy changes and adiabatic boundaries except at the heat exchangers:

$$Q_{cond} = Q_{evap} + W_{comp} \quad (1)$$

$$COP_H = \frac{Q_{cond}}{W_{comp}} \quad (2)$$

$$COP_C = \frac{Q_{evap}}{W_{comp}} \quad (3)$$

For the cascades (C3, C4), the balance is applied sequentially: the Stage-1 condenser (gas-cooler) output drives the Stage-2 evaporator, supplemented where required by spray-dryer exhaust heat:

$$Q_{evap,2} = Q_{cond,1} + \Delta Q_{waste} \quad (4)$$

where $\dot{Q}_{cond}$, $\dot{Q}_{evap}$ and $\dot{W}_{comp}$ are the condenser (gas-cooler) duty, evaporator duty and compressor shaft power (kW); COP_H and COP_C are the heating and cooling COPs; $\dot{Q}_{evap,2}$ and $\dot{Q}_{cond,1}$ are the Stage-2 evaporator and Stage-1 condenser duties; and $\Delta\dot{Q}_{waste}$ is supplementary heat from exhaust air at 90–95 °C (kW). $\dot{Q}_{evap}$ is fixed by the cooling requirement (879 kW), limited by the heat that Stage 1 can usefully deliver; $\dot{W}_{comp}$ follows from the cycle COP (Section 3.3) and $\dot{Q}_{cond}$ from Equation (1). $\Delta\dot{Q}_{waste}$ is calculated, not assumed: it is zero at the cycle COPs for C3 and C4, and non-zero values arise only in the sensitivity cases (Section 3.4.2). For $\Delta\dot{Q}_{waste}$ = 0 the combined heating COP of the cascade is:

$$(C3):\ COP_{cas} = \frac{COP_1 \, x \, COP_2}{(COP_1 + COP_2 - 1)} \quad (5)$$

The COP boundary is the compressors only. The heating COP of a configuration is the heat delivered to the process divided by the shaft power of all stages including the MVR; for C4, $(\dot{Q}_{c2} + \dot{W}_{MVR})/(\dot{W}_1 + \dot{W}_2 + \dot{W}_{MVR})$ = (2,688.9 + 290.8)/2,303.9 = 1.29. The MVR is treated as an adiabatic steam compressor:

$$WMVR = m_{steam} \, x \frac{H_2S - H_1}{\eta is} \quad (6)$$

where $\dot{m}_{steam}$ is the steam flow through the compressor (kg/s), H_1 the enthalpy of saturated suction steam at 5.013 bar (2,748.2 kJ/kg), H_{2S} the enthalpy after isentropic compression to 13.013 bar (2,948.3 kJ/kg) and η_{is} = 0.70. For 4,000 kg/h of delivered steam with a 25 °C spray-water desuperheater (0.094 kg/s; Table S6), $\dot{m}_{steam}$ = 1.017 kg/s and $\dot{W}_{MVR}$ = 1.017 × (2,948.3 – 2,748.2)/0.70 = 290.8 kW; the 440 kW nameplate corresponds to 1.54 kg/s and is not used.

2.5. Exergy analysis (second law)

The exergy rate of a heat transfer at temperature T relative to the dead state T_0 is:

$$E_x Q = \left(1 - \frac{T_0}{T}\right) x \, Q \quad (T > T_0)$$

$$E_x Q = \left(\frac{T_0}{T} - 1\right) x \, Q \quad (T < T_0) \quad (7)$$

Exergy destruction and second-law (exergetic) efficiency of each component k are [14], [15]:

$$\dot{I}_k = E_{x,in,k} - E_{x,out,k} = T_0 \, x \, \dot{S}_{gen,k} \quad (8)$$

$$\psi = \frac{\dot{E}_{x,out,total}}{\dot{E}_{x,in,total}} \quad (9)$$

$$y^*_k = \frac{\dot{I}_k}{\dot{E}_{x,in,total}} \quad (10)$$

where T_0 = 298.15 K is the dead-state temperature (annual mean ambient temperature at the site); $\dot{I}_k$ and $\dot{S}_{gen,k}$ are the exergy destruction and entropy generation rates of component k; $\dot{E}x_{in,k}$ and $\dot{E}x_{out,k}$ its exergy inflow and outflow (kW); ψ is the system exergy efficiency; and y^*k is the exergy destruction ratio. Stream exergies use IAPWS-IF97 and CoolProp 8.0.0 data, and the fuel exergy of natural gas is 1.04 times its LHV [24].

Table 3. Treatment of each stream in the exergy balance.

Stream	Role	Exergy Expression	Baseline Value
Natural gas	Input	1.04 × LHV × $\dot{m}_{gas}$ (LHV 10.5 kWh/m^3, η_{boiler} 0.85)	3,645.7 kW
Electricity	Input	$\dot{W}_{el}$ (pure exergy)	274.7 kW (chiller, COP 3.2)
Exhaust-air heat	Input, if used	$(1 - T_0/T_w)\,\Delta\dot{Q}_{waste}$	0 for the baseline
Steam 12 barg	Product	$\dot{m}[(h - h_0) - T_0(s - s_0)]$; 855.2 kJ/kg	950.2 kW at 1.111 kg/s
Chilled water 6/12 °C	Product	$\dot{Q}_{ch}\,(T_0/\bar{T}_{ch} - 1)$; $\bar{T}_{ch}$ = 282.14 K	49.9 kW at 879 kW
Hot water 70–85 °C (C2)	Product	$\dot{Q}\,(1 - T_0/T_{hw})$	0.1496 kW per kW
Steam 4 barg (C3)	Product	as for 12 barg; 719.6 kJ/kg	-

The system boundary is the utility side described in Section 2.1. The inputs crossing the boundary are natural gas, electricity and, where used, exhaust-air heat at T_w = 365.65 K; the products are the steam (reference state: saturated liquid water at 25 °C), the chilled water and, for C2, the hot water (Table 3). Streams passing between components appear once as an outlet and once as an inlet and cancel, so that the system destruction equals the sum of the component destructions.

$$E_{xF} = 1.04 m_{gas} LHV + W_{el} + \left(1 - \frac{T_0}{T_w}\right) \Delta Q_{waste} \tag{11}$$

$$\dot{E}_{xP} = \dot{m}_s[(h - h_0) - T_0(s - s_0)] + \dot{Q}_{ch}\left(\frac{T_0}{\overline{T}_{ch}} - 1\right) + \dot{Q}_{hw}\left(1 - \frac{T_0}{\overline{T}^*_{hw}}\right) \tag{12}$$

$$\dot{I}_{sys} = \dot{E}_{xF} - \dot{E}_{xP} = \sum_k \dot{I}_k \tag{13}$$

2.6. COP thermodynamic consistency validation

Before use, each COP is compared with the Lorenz limit of the actual heat source and sink, which no real vapour-compression cycle can exceed; for streams with temperature glide this limit, not the isothermal Carnot COP, is the relevant bound [25]. The Carnot COP is retained as a reference:

$$COP_{Carnot,H} = \frac{TH}{(TH - TC)} \tag{14}$$

where T_H and T_C are the absolute condenser (or gas-cooler outlet) and evaporator temperatures (Table 2). The Lorenz limit uses the thermodynamic mean temperature of each stream, $\bar{T} = \Delta h/\Delta s$, with and without a 5 K approach temperature difference ΔT_a at each exchanger:

$$COPL = \frac{\overline{T}_H + \Delta T_a}{\left(\overline{T}_H + \Delta T_a\right) - \left(\overline{T}_C - \Delta T_a\right)} \tag{15}$$

and the second-law efficiency of a cycle relative to this limit is:

$$\eta_2 = \frac{COP_{,actual}}{COP_L} \tag{16}$$

where COP_{actual} is the design (vendor) or cycle COP; η_2 > 100% identifies a physically inconsistent COP. Because a limit shows that a value is impossible but not what the correct value is, the COP used in the analyses is calculated for each stage from a vapour-compression cycle: evaporating and condensing temperatures equal the process temperatures ∓ 5 K, suction superheat is 5 K, the liquid is subcooled to the sink inlet temperature + 5 K, η_{is} = 0.70 (0.65–0.80 tested), and the CO_2 cycle has an internal heat exchanger (IHX) of effectiveness 0.8 [26], [27].

2.7. Configuration-selection framework

Existing selection approaches weight several indicators in one score. The framework used here instead applies two sequential tests: (i) delivery-envelope compliance as a pass/fail gate, and (ii) ranking of the compliant options by Lorenz-consistent exergy efficiency, with a qualitative complexity index reported alongside. A configuration is fully compliant when it directly supplies the required utilities (here 12 barg/191 °C saturated steam and 6 °C chilled water), partially compliant when it meets the cooling duty but needs additional equipment to reach the steam condition, and non-compliant when it cannot deliver the heating or cooling duty on its own. The complexity index (number of thermodynamic stages plus auxiliary units such as an MVR) indicates integration, control and maintenance effort,

not cost. In the Results, each configuration is reported under three separate headings: (A) thermodynamic performance, (B) process feasibility and (C) compliance with the required 12 barg steam (Section 3).

2.8. Baseline reference calculation and model validation

The baseline is the existing boiler–chiller system, and its duties were calculated rather than assumed. The peak boiler duty follows from the steam flow, and the enthalpy rise from feedwater to saturated steam:

$$Q_{boiler,peak} = m_{steam} x(h_g - h_f) = 4000\ x \frac{2{,}786.5 - 104.8}{3{,}600} = 2{,}979.7\ kW \quad (17)$$

where $\dot{m}_{steam}$ = 4,000 kg/h, h_f = 104.8 kJ/kg (feedwater, 25 °C) and h_g = 2,786.5 kJ/kg (saturated steam, 13 bar abs.), both from IAPWS-IF97. The chiller duty is the nameplate 879 kW at 6/12 °C. Annual energy is $E = P_{peak}$ × 7,680 h × LF, with the load factors LF of Table 4.

Three checks against operating data were applied. First, the peak duty of 2,980 kW agrees with the 4 t/h rating within 1%. Second, the annual useful steam energy (3,614,212 kWh/yr) implies 4.25–4.41 GWh/yr of fuel at the nameplate efficiency of 82–85%, 1.2–4.9% above the 4.20 GWh/yr from the metered 400,000 m^3; the metered fuel thus corresponds to an effective efficiency of 86.05%, used to convert gas volumes in Tables 6 and 11 (0.85 is used for the design-point fuel exergy; 1.2% difference). The steam energy corresponds to a load factor of 3,614,212/(2,980 × 7,680) = 0.158 (about 632 kg/h). Third, the annual cooling energy cannot exceed 879 kW × 7,680 *h* = 6,750,720 kWh/yr, so the compressor electricity at COP 3.2 cannot exceed 2,109,600 kWh/yr, against 3,870,720 kWh/yr recorded; the difference

Table 4. Complete input data of the model.

Parameter	Value	Reference
Steam duty	4,000 kg/h, saturated, 12 barg (13.013 bar a)	Plant rating
Feedwater temperature	25 °C (h = 104.8 kJ/kg)	Plant Record
Dead state	T0 = 298.15 K, p0 = 1.01325 bar	Adopted in this study
Natural gas	400,000 m^3/yr; LHV 10.5 kWh/m^3; fuel exergy 1.04 × LHV	Plant Record
Boiler efficiency	82–85% (0.85 in design-point balances); 0.8605 effective (annual gas basis, derived)	Nameplate
Chiller	250 TR = 879 kW, R134a, 6/12 °C, COP 3.2	Nameplate
Operating time	320 d × 24 h = 7,680 h/yr	Calculated
Boiler load factor	0.158	Derived from gas meter
Chiller load factor	0.90	Adopted upper bound
Fluids, C1 / C2	R134a / R1233zd(E)	Design input of this study
Fluids, cascade	R-744 (Stage 1) / HFO-1336mzz(Z) (Stage 2)	Design input of this study
Compressor isentropic efficiency	0.70 (all stages incl. MVR)	Adopted in this study
Minimum approach; suction superheat	5 K; 5 K	Adopted in this study
CO_2 gas-cooler pressure; IHX effectiveness	224 bar; 0.8	Adopted in this study
Grid emission factor; gas factor	0.88 t CO_2/MWh; 0.181 t CO_2/MWh (LHV)	Adopted values; gas factor = recorded 760 t ÷ 4,200 MWh

(at least 1.76 GWh/yr) cannot be allocated without sub-metering and is excluded. The boiler baseline is therefore validated against metered gas, whereas the chiller baseline is bounded rather than validated.

The calculation is checked at three levels: (a) verification (energy balances close in every component, $\Sigma \dot{I}k = \dot{I}sys$ to below 10−6 kW, and spreadsheet and script agree); (b) comparison with plant data, as above; and (c) comparison with published stage-level efficiencies (Section 3.7.2). Because neither C3 nor C4 is installed, these checks verify the calculation and test its plausibility but are not an experimental validation of the heat pump models, which are instead tested against the Lorenz limit (Sections 2.6 and 3.3) and by sensitivity analysis (Section 3.5).

3. Results and Discussion

Results follow the workflow of Section 2.2. Each configuration is assessed under three separate headings: (A) thermodynamic performance (heating COP and exergy efficiency ψ); (B) process feasibility (what is delivered, the share of the 4,000 kg/h steam duty it covers, and the heat or boiler capacity it still needs from outside); and (C) compliance with the required 12 barg (191 °C) steam. Heading (C) is decided by (B) alone and does not depend on ψ.

3.1. Baseline utility system reference

Table 5 summarizes the baseline derived in Section 2.8; only the compressor electricity of the chiller enters the heat pump comparison.

3.2. Comparative energy balance of the four configurations

Table 6 places all configurations on one service basis, with the steam duty following the gas meter (load factor 0.158). The annual electricity of each heat pump is its design-point compressor power (Table 2) multiplied by 7,680 h/yr and by the same load factor of 0.158, because the heat pump is assumed to follow the steam demand (e.g. 1,814.1 kW × 7,680 h × 0.158 = 2.201 GWh/yr for C3). The remaining chiller covers the cooling not displaced, at COP 3.2 and an assumed load factor of 0.90, which changes the absolute site electricity but not the electricity a configuration adds relative to the baseline. Residual gas falls from 400,000 m^3/yr to 368,805 (C1), 252,332 (C2), 70,000 (C3) and 0 m^3/yr (C4), since C1 and C2 are confined to hot water and C3 to the 4 barg share, while site electricity rises from 1.899 to 4.438 GWh/yr.

State points of every stage (pressure, temperature, enthalpy, entropy, refrigerant flow) are given in Supplementary Tables S2–S6. Two bear on feasibility (heading B): the CO_2 stage, which must reject heat at 90 °C to drive the 85 °C Stage-2 evaporator, reaches a discharge temperature of 290.5 °C, far above the limits of current CO_2 compressors; and the HFO stage condenses at 157 °C, 14 K below its critical temperature, with a two-phase discharge (x = 0.92) unless the suction superheat is at least 10 K (COP about 2.73). Both require confirmation by compressor manufacturers.

Table 5. Baseline (existing) utility system energy balance.

Parameter	Existing Boiler	Existing Chiller
Nominal capacity/load (kW)	2,980 (peak)	879
Load factor	0.158 (from the gas meter)	0.90 (adopted upper-bound value)
Annual useful energy (kWh/yr)	3,614,212	6,750,720 at LF 1.00; 6,075,648 at LF 0.90
Annual fuel/electricity input	400,000 m^3 gas	3,870,720 kWh (recorded, refrigeration system)
Compressor electricity at COP 3.2 (kWh/yr)	–	2,109,600 (LF 1.00); 1,898,640 (LF 0.90)
Recorded electricity not explained by the compressor (kWh/yr)	–	1,761,120 (LF 1.00); 1,972,080 (LF 0.90)

Table 6. Energy balance of all configurations on one service basis (boiler load factor 0.158, chiller load factor 0.90 [assumed], cycle COPs of Section 3.3).

Quantity	Baseline	C1	C2	C3	C4
Residual gas (m^3/yr)	400,000	368,805	252,332	70,000	0
HP electricity (GWh/yr)	–	0.081	0.521	2.201	2.796
Site electricity, HP + remaining chiller (GWh/yr)	1.899	1.917	2.166	3.869	4.438
Heating COP of the HP (–)	–	3.47	2.56	1.34	1.29

3.3. COP validation and system-level exergy analysis

The isothermal Carnot COPs (C1: 5.05; C2: 4.90; CO_2 stage: 4.04) are not the correct bound for a sink heated through a range (feedwater 25 → 75 °C; hot water 70 → 85 °C) and a source cooled through a range (chilled water 12 → 6 °C). The Lorenz limits (Table 7) are 7.99 (C1), 5.12 (C2), 4.71 (CO_2 stage) and 8.82 (HFO stage) without approach and 6.50, 4.53, 4.22 and 7.35 with a 5 K approach. The design COPs of C1 (5.1) and of the cascade stages (3.5, 2.7) are admissible; that of C2 (5.3) exceeds the limit even without approach and is inadmissible.

The COP used in the analysis is therefore calculated from the cycle (Supplementary Tables S2–S5). For C2 the cycle gives 2.56 (2.45–2.79 for η_{is} = 0.65–0.80); even an ideal compressor gives only 3.23 for a lift from about 1 °C to 90 °C, so a higher value would need a different cycle (e.g. two-stage with economizer or a zeotropic mixture) specified by the vendor. C1 gives 3.47 (3.30–3.82). The CO_2 stage gives 1.68 (1.64–1.78) against the design 3.5, because the 90 °C gas-cooler outlet needed by Stage 2 removes much of the transcritical benefit [26]–[28]; the HFO stage gives 2.62 (2.51–2.79), close to the design 2.7 (Table S7). The heating COP thus ranks C1 (3.47) > C2 (2.56) > C3 (1.34) > C4 (1.29), whereas the vendor values would have ranked C2 above C1, which substantiates the caution of Bellos et al. [12] that quoted COPs must be re-referenced to site temperatures.

Table 8 summarizes the system-level balances (Equations (7)–(13), Table 3) at the design point (4,000 kg/h of steam, 879 kW of chilled water, cycle COPs). ψ rises from 25.5% (baseline) to 27.4% (C1), 29.1% (C2), 34.5% (C3, independent model) and 42.2% (C4). Because the products differ (C3 raises 82.5% of the steam at 4 barg), the ψ values compare utility systems that meet the stated duty, not heat pump units at equal supply temperature, and are read together with the compliance assessment (Section 3.6). In the baseline, gas burned at a flame temperature of the order of 2,000 K is degraded across more than 1,700 K before reaching 191 °C steam; each configuration replaces more of this duty by electricity, leaving only heat-exchanger and compressor losses. The baseline value is of the same order as the

Table 7. Validation of design COP values against the Lorenz limit and comparison with the cycle COP (η_{is} 0.70); $\eta_{2,0}$ and $\eta_{2,5}$ refer to the limit without and with a 5 K approach.

Configuration/Stage	Design COP	η2,0 Design	η2,5 Design	Cycle COP	η2,0 Cycle	η2,5 Cycle
C1-Preheater HP	5.1	64%	78%	3.47	43%	53%
C2-SHC-HP	5.3	104%	117%	2.56	50%	57%
C3/C4 Stage 1, CO_2 (0 → 90 °C)	3.5	74%	83%	1.68	36%	40%
C3/C4 Stage 2, HFO (90 → 4 barg steam)	2.7	31%	37%	2.62	30%	36%
Cascade, 0 °C → 4 barg steam	1.82	57%	60%	1.34	42%	44%

Table 8. System-level exergy balance of the baseline and C1–C4 (design point, cycle COPs, T_0 = 298.15 K).

System	Ex_{in} (kW)	Ex_{out} (kW)	$\dot{I}$ (kW)	ψ (%)
Baseline (Boiler+Chiller)	3,920.4	1,000.1	2,920.3	25.5
C1-Preheater	3,651.3	1,000.1	2,651.2	27.4
C2-SHC-HP	2,794.1	813.9	1,980.2	29.1
C3-Cascade HTHP	2,536.5	875.8	1,660.7	34.5
C4-Cascade HTHP+MVR	2,367.4	1,000.1	1,367.3	42.2

26.1% of the boiler alone and the 27–32% reported for a natural-gas-fired utility boiler [29]. Figure 2 shows the exergy flows.

3.4. Component-level irreversibility and Independent model of C3

3.4.1. Component-Level Irreversibility

Table 9 decomposes the destruction by component. In the baseline the boiler dominates (2,695.5 kW; component efficiency 26.1%; 92.3% of the total), whereas the chiller destroys

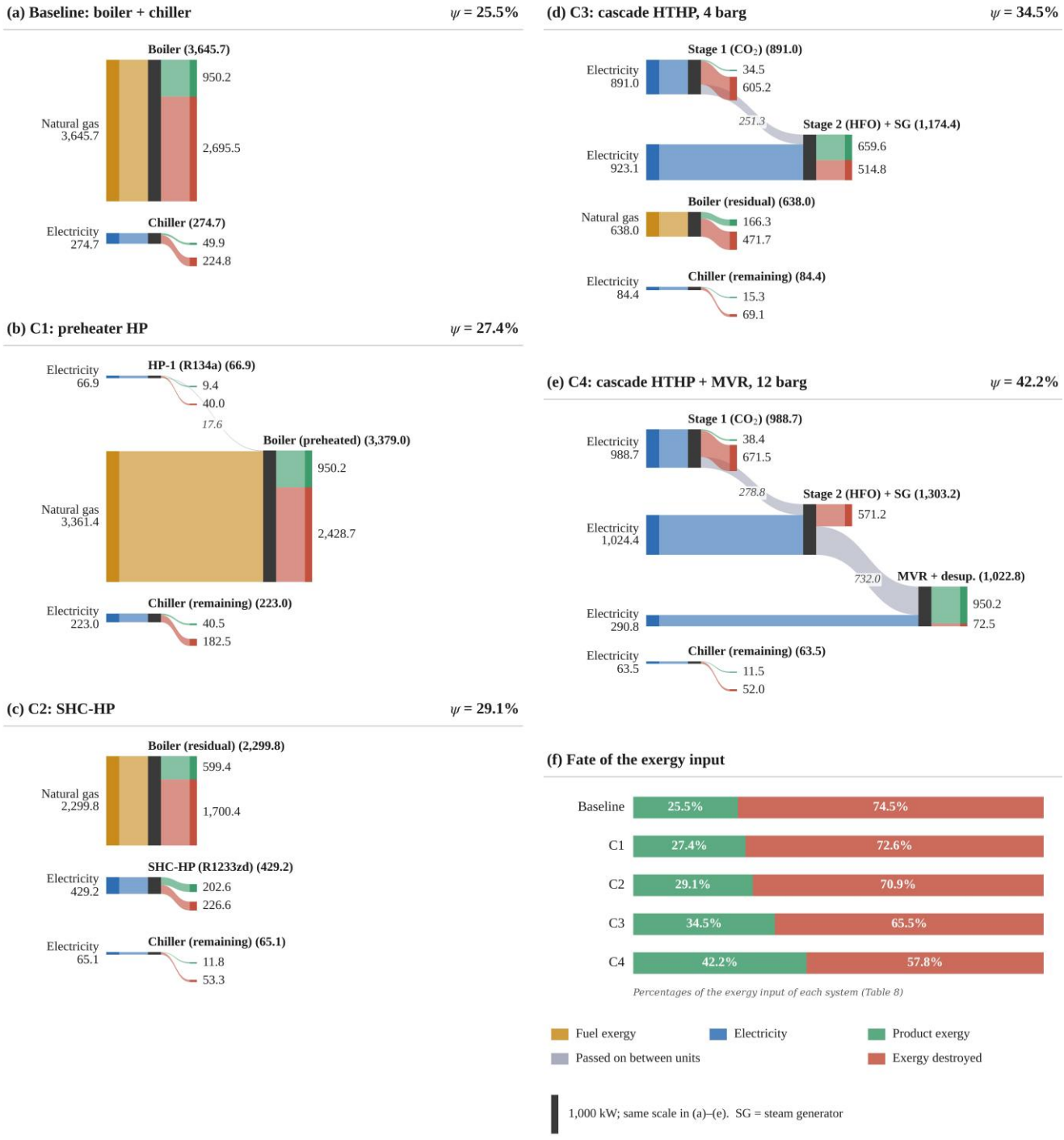


Figure 2. Grassmann diagrams of the baseline (a) and of C1 (b), C2 (c), C3 (d) and C4 (e) at the design point (cycle COPs, T_0 = 298.15 K); band width is proportional to the exergy rate (kW) on one scale. Fuel exergy is orange, electricity blue, exergy passed between units grey, product green and destruction red; values beside each unit are its input, product and destroyed exergy (Table 9). Panel (*f*): product (ψ) and destroyed shares of each system's exergy input (Table 8). SG: steam generator.

Table 9. Component-level exergy balance (design point, cycle COPs, kW); $\Sigma \dot{I}_k$ equals the system $\dot{I}$ of Table 8 for every configuration.

Component / Configuration	Ex_{in} (kW)	Ex_{out} (kW)	$\dot{I}$ (kW)	ψ_k (%)	Share of system $\dot{I}$ (%)
Baseline — boiler	3,645.7	950.2	2,695.5	26.1	92.3
Baseline — chiller	274.7	49.9	224.8	18.2	7.7
C1 — boiler (with preheat exergy)	3,379.0	950.2	2,428.7	28.1	91.6
C1 — HP-1	66.9	27.0	40.0	40.3	1.5
C1 — remaining chiller	223.0	40.5	182.5	18.2	6.9
C2 — boiler	2,299.8	599.4	1,700.4	26.1	85.9
C2 — HP-2 (SHC-HP)	429.2	202.6	226.6	47.2	11.4
C2 — remaining chiller	65.1	11.8	53.3	18.2	2.7
C3 — residual boiler	638.0	166.3	471.7	26.1	28.4
C3 — stage 1 (CO_2)	891.0	285.8	605.2	32.1	36.4
C3 — stage 2 (HFO) + steam generator	1,174.4	659.6	514.8	56.2	31.0
C3 — remaining chiller	84.4	15.3	69.1	18.2	4.2
C4 — stage 1 (CO_2)	988.7	317.2	671.5	32.1	49.1
C4 — stage 2 (HFO) + steam generator	1,303.2	732.0	571.2	56.2	41.8
C4 — MVR + desuperheater	1,022.8	950.2	72.5	92.9	5.3
C4 — remaining chiller	63.5	11.5	52.0	18.2	3.8

224.8 kW (7.7%) at a low efficiency (18.2%) because chilled water carries little exergy per unit heat. Displacing boiler duty therefore gains most: C3 and C4 raise ψ by 9.0 and 16.7 points, C1 and C2 by 1.9 and 3.6 points, and the boiler share of the destruction falls from 92.3% to 28.4% (C3) and 0% (C4).

In the cascades, the CO_2 stage reaches 32.1% and the HFO stage with steam generator 56.2%; the lower CO_2 value reflects the 90 °C gas-cooler outlet imposed by Stage 2. Splitting the lift keeps the pressure ratios at 6.4 (CO_2) and 4.6 (HFO) at the cost of an intermediate temperature difference, a trade-off consistent with Dong and Wang [17] and the zeotropic cascades of [30], [31]. The MVR destroys only 72.5 kW (5.3%; component efficiency 92.9%) but is essential for 12 barg steam, and in C4 no component causes more than about half of the destruction (Stage 1, 49.1%).

3.4.2. Independent model of C3 and Sensitivity analysis

C3 is solved with its own balance, not derived from C4: removing the MVR from C4 would omit the fuel of the boiler that C3 retains for 17.5% of the steam duty (70,000 m^3/yr, Table 6) and would credit 12 barg steam exergy to a product delivered at 4 barg. The Stage-2 duty is set by the 4 barg steam flow of C3 alone (f4 = 0.825) and Equation (4) is applied without any value from C4. C3 then needs Stage-2 and Stage-1 evaporator duties of 1,500.0 and 609.0 kW (C4: 1,664.5 and 675.8 kW), a residual boiler fuel input of 613.5 kW (LHV) and a total electricity input, including the remaining chiller, of 1,898.5 kW (C4: 2,367.4 kW).

With the cycle COPs, ψ is 34.5% for C3 against 42.2% for C4 (7.7 points); with the design COPs, 45.1% against 58.0%. A 36-case grid was computed over the uncertain inputs of C3: Stage-1 COP ∈ {1.68, 2.5, 3.5}, Stage-2 COP ∈ {2.2, 2.62, 2.7, 3.2} and f4 ∈ {0.7, 0.825, 1.0} (Supplementary Table S1). ψ ranges from 31.6% to 60.0% for C3 and from 40.4% to 62.6% for C4; C3 never exceeds C4, and the difference lies between 2.6 and 20.5 points. The smallest difference occurs only when both COPs are highest and C3 serves all the steam, which needs about 789 kW of supplementary heat not documented for the plant. At f_4 = 0.825, C3 needs 0, 295 and 435 kW of supplementary heat at the cycle COPs, the design COPs (C4: about 462 kW) and COPs of 3.5/3.2, respectively.

3.5. Sensitivity to COP and isentropic-efficiency assumptions

A one-at-a-time sensitivity analysis is applied to the quantities that the governing equations constrain exactly, so that no unstated state-point assumptions are introduced (Supplementary Figure S1). First, the cycle COPs for ηis = 0.65–0.80 (Section 3.3; Table S7) remain below their Lorenz limits; the COP of C2 stays between 2.45 and 2.79, far below the vendor value of 5.3. Replacing the design COPs by the cycle COPs changes ψ by 0.2 (C1), 3.2 (C2), 10.6

Table 10. Configuration-selection framework applied to C1–C4, with (A) thermodynamic performance, (B) process feasibility and (C) compliance with the required 12 barg steam shown separately; *sensitivity cases.

Configuration	(A) ψ design point (%)	(A) Heating COP (cycle)	(B) What is delivered	(B) Share of steam duty at 12 barg	(B) External need	(C) Delivery-envelope compliance	Complexity	Most Suitable Application
C1-Pre-heater HP	27.4	3.47	Feedwater at 75 °C; no steam	100% from boiler	Boiler retained	Non-compliant (steam); cooling met	1	Fast, low-risk reduction; boiler retained
C2-SHC-HP	29.1	2.56	Hot water 70–85 °C; no steam	100% from boiler	Boiler retained	Non-compliant (steam); cooling met	1	Hot-water-dominated processes
C3-Cascade HTHP	34.5	1.34	4 barg/152 °C steam, 82.5% of duty	17.5% from boiler	Boiler or booster; exhaust heat 0–435 kW*	Partially compliant (≤4 barg)	2	Medium-pressure users; backup for header
C4-Cascade HTHP+MVR	42.2	1.29	12 barg/191 °C steam, 100% of duty	100%	Exhaust heat 0–462 kW*	Fully compliant (12 barg)	3	Full boiler replacement; Scope 1 eliminated

(C3) and 15.8 (C4) points (design-COP values 27.6, 32.3, 45.1 and 58.0%) without changing the ordering.

Second, the annual electricity of C4 scales inversely with the effective cascade COP: a ±10% variation moves it between 2.54 and 3.11 GWh/yr around 2.80 GWh/yr. Third, the MVR power ($\propto 1/\eta is$) ranges from 339 kW at 60% to 254 kW at 80% against 291 kW at 70%, without affecting the compliance of C4, which is set by the pressure ratio. Fourth, supplying 0–100% of the 1,664.5 kW Stage-2 evaporator duty of C4 from exhaust air would lower the Stage-1 power from 988.7 kW to zero but raise the remaining-chiller power from 63.5 to 274.7 kW.

The ranking of Table 8 is therefore robust to plausible COP and isentropic-efficiency uncertainty: the perturbations shift absolute energy demand but do not reorder the configurations, and every cycle COP stays below its Lorenz limit. A probabilistic (Monte Carlo) propagation onto ψ is left for future work.

3.6. Applying the configuration-selection framework

Table 10 applies the framework of Section 2.7. Ranked by ψ, C4 (42.2%) leads C3 (34.5%), C2 (29.1%) and C1 (27.4%). Ranked by compliance, only C4 meets the 12 barg header; C3 is partially compliant, and C1 and C2 are non-compliant for steam although they take over part of the chiller duty. The rankings agree here but are independent: compliance is decided by the final saturation pressure, so C3 fails the gate whatever its ψ, even where the sensitivity grid brings it within 2.6 points of C4. Since only C4 passes Step 1, Step 2 reduces to confirming its ψ and complexity; it discriminates when several configurations pass, e.g. for a lower-pressure header.

3.7 Discussion

3.7.1. What Explains the result

The ranking baseline < C1 < C2 < C3 < C4 in ψ (Table 8) arises because each step replaces fuel exergy, destroyed mainly in combustion, by electricity, which is pure exergy (Table 9); the 7.7-point gap between C3 and C4 arises because the MVR destroys little exergy (93% component efficiency) while removing the residual boiler. The heating COP follows the opposite order because it follows the temperature lift of each duty, as the Lorenz limits predict (Table 7).

3.7.2. Comparison with existing work

Walmsley et al. [5] reported a 51.5% reduction in thermal energy use for milk powder production; their boundary (whole process) and measure (energy) differ from the present

ones, so the results are complementary rather than comparable. The 60–70% exergy efficiencies of cascade HTHPs alone [14], [15] correspond at stage level to the present 32.1% (CO_2 stage, lower because of the 90 °C gas-cooler outlet) and 56.2% (HFO stage with steam generator), not to the whole-utility values of Table 8. The baseline agrees with the published boiler value [29], and the COP result is consistent with [12]. No published whole-utility exergy efficiency was found for this combination of duties.

3.7.3. Limitations

Applicability: a 12 barg, 24 h/day steam duty with coincident cooling and a utility-side boundary. Conditions: steady state at the design point, no part-load behaviour, η_{is} = 0.70 and a 5 K approach. Reproducibility: all inputs in Table 4 and all state points in Supplementary Tables S2–S6. Stability: Section 3.5 and Table S1. Range: other temperature lifts require Equations (1)–(16) to be solved again. Data: the chiller load factor and exhaust-air heat are not measured, and the CO_2 gas-cooler pressure and IHX effectiveness are assumptions on which the cycle COPs rest.

3.7.4. Supplementary heat, emissions and future work

Supplementary heat at the Stage-2 evaporator (Equation (4)) is not needed at the cycle COPs but reaches 295–789 kW in the sensitivity cases, and its only candidate source, spray-dryer exhaust air at 90–95 °C, has not been measured. Operational emissions are given in Table 11. The Scope-1 elimination of about 760 t CO_2/yr in C4 does not by itself imply lower total emissions: at the adopted grid factor of 0.88 t CO_2/MWh the totals of C3 and C4 increase, and they would decrease only below break-even factors of 0.32 (C3) and 0.30 t CO_2/MWh (C4), which do not depend on the chiller load factor.

Future work. Four items would reduce the uncertainty: (i) measurement of the spray-dryer exhaust flow and temperature; (ii) manufacturer confirmation that the CO_2 stage (discharge about 290 °C) and HFO stage (condensing at 157 °C) can be built; (iii) part-load and dynamic simulation; and (iv) techno-economic and life-cycle assessment. Practical difficulties include integrating a 12 barg MVR steam system with the existing header and controlling two coupled refrigerant circuits.

3.8. Practical implications and generalization

Where spray drying requires 12 barg steam, C1 and C2 are transitional rather than complete solutions: they reduce boiler load and part of the chiller duty ahead of a later cascade HTHP+MVR retrofit. C3 delivers only 4 barg steam whatever its ψ, a compliance risk easily missed in an efficiency-first evaluation. The minimum delivery envelope should therefore be fixed before configurations are compared on efficiency, cost or emissions.

The framework is not specific to dairy processing; its criteria derive from process requirements and apply to any industry with coincident heating and cooling and a defined steam pressure. Dairy spray drying is demanding because it combines continuous coincident loads (2,980 kW steam and 879 kW chilled water for 7,680 h/yr), a 12 barg (191 °C) requirement above the 100–160 °C range of most commercial HTHPs [13] (research cycles reach 200 °C [30]–[32]) and hygienic constraints requiring indirect steam heating. Where most heat demand lies below 200 °C, as in brewing, pasteurization and textile dyeing [1], [2], C3 or C2 becomes preferable. Screening criteria for other sites are a sufficient cooling-to-heating ratio (0.29 here), substantial overlap of the two demands (7,680 h/yr) and a defined minimum delivery pressure; their duties and conditions can then be substituted into Equations (1)–(17).

Table 11. Operational CO_2 emissions (Scope 1 + Scope 2), t CO_2/yr; meter-anchored load, cycle COPs. Scope 1: 4,200 MWh × 0.181 t CO_2/MWh = 760 t; Scope 2: electricity × 0.88 t CO_2/MWh.

Quantity	Baseline	C1	C2	C3	C4
Total operational (t CO_2/yr)	2,431	2,388	2,386	3,538	3,904
Change vs baseline (t CO_2/yr)	–	−43	−45	+1,107	+1,475
Change (%)	–	−1.8	−1.9	+45.5	+60.7
Break-even grid factor (t CO_2/MWh)	–	3.19	1.05	0.32	0.30

4. Conclusions

This study compared a boiler–chiller baseline and four HP configurations (C1–C4) for a dairy spray-drying utility requiring 12 barg steam and 250 TR of cooling. One numbered conclusion is given for each objective. ψ rises from 25.5% (baseline) to 27.4% (C1), 29.1% (C2), 34.5% (C3) and 42.2% (C4), while the heating COP falls from 3.47 (C1) to 1.29 (C4). The rise is explained by the progressive replacement of combustion exergy by electricity. The values are lower than the 60–70% reported for cascade HTHPs alone because the product here is the whole utility duty; the ordering agrees with [14], [15]. The vendor COP of the SHC-HP (5.3) exceeds its Lorenz limit (5.12) and was replaced by a cycle-based 2.56; the C1 value (5.1) is admissible, but the cycle gives 3.47. A limit shows that a value is impossible but not what the correct value is, so a cycle model is needed in addition; unlike the common adoption of quoted COPs cautioned against in [12], an inadmissible value is replaced before it enters the comparison. Independent modelling gives 34.5% for C3 against 42.2% for C4 (7.7 points; 2.6–20.5 points across the sensitivity grid). The two rankings agree here but are independent: compliance is fixed by the final steam pressure, whereas ψ of C3 ranged from 31.6% to 60.0% without changing its 4 barg limit. This differs from single-score approaches [6], [17], in which high efficiency can offset a delivery shortfall. Only C4 supplies 12 barg (191 °C) steam; C3 delivers 4 barg (152 °C), and C1 and C2 supply no steam. This is set by the final saturation pressure, not by efficiency, consistent with the steam-range delivery of about 150 °C demonstrated experimentally [11]. The compliance of C4 is conditional on manufacturer confirmation of its compressors (CO_2 discharge 290.5 °C; HFO condensing at 157 °C) and, at higher COPs, on supplementary heat. A two-step procedure, delivery envelope first and Lorenz-consistent performance second, is proposed for use before techno-economic assessment. Here it excludes C1–C3 for the 12 barg duty and shows that the Scope-1 elimination of C4 (about 760 t CO_2/yr) lowers total operational emissions only below a grid factor of about 0.30 t CO_2/MWh; life-cycle emissions were not computed. The results are specific to this case and its assumptions (Table 4) and should be confirmed with measured plant data.

Acknowledgements

The authors thank the Ministry of Higher Education, Science, and Technology of the Republic of Indonesia (Kemdiktisaintek-RI) for funding this research through the BIMA (Basis Informasi Penelitian dan Pengabdian kepada Masyarakat) research grant program, PT Lautan Natural Krimerindo for providing operational and process data, and Universitas Muhammadiyah Malang for its academic support and research collaboration.

Declaration of Generative AI and AI-Assisted Technologies in the Writing Process

The authors used ChatGPT (OpenAI) solely to assist with language editing and improve the clarity and readability of the manuscript. All scientific analyses, calculations, interpretations, and conclusions were independently developed and verified by the authors. All AI-assisted text was critically reviewed and revised by the authors, who take full responsibility for the content of the published article.

References

[1] International Energy Agency, "Can low-temperature heat in factories be electrified competitively?" Paris, France: IEA, 2025. [Online]. Available: https://www.iea.org/commentaries/can-low-temperature-heat-in-factories-be-electrified-competitively

[2] F. Faraldo and P. Byrne, "A review of energy-efficient technologies and decarbonating solutions for process heat in the food industry," *Energies*, vol. 17, no. 12, Art. no. 3051, 2024, doi: 10.3390/en17123051.

[3] E. Vieren *et al.*, "The potential of vapor compression heat pumps supplying process heat between 100 and 200 °C in the chemical industry," *Energies*, vol. 16, no. 18, Art. no. 6473, 2023, doi: 10.3390/en16186473.

[4] J. Zuberi, A. Hasanbeigi, and W. R. Morrow III, "Bottom-up assessment of industrial heat pump applications in U.S. food manufacturing," *Energy Convers. Manage.*, vol. 272, Art. no. 116349, 2022, doi: 10.1016/j.enconman.2022.116349.

[5] T. G. Walmsley, M. J. Atkins, M. R. W. Walmsley, M. Philipp, and R.-H. Peesel, "Process and utility systems integration and optimisation for ultra-low energy milk powder production," *Energy*, vol. 146, pp. 67–81, 2018, doi: 10.1016/j.energy.2017.04.142.

[6] F. Schlosser, S. Zysk, T. G. Walmsley, L. Kong, B. Zühlsdorf, and H. Meschede, "Break-even of high-temperature heat pump integration for milk spray drying," *Energy Convers. Manage.*, vol. 291, Art. no. 117304, 2023, doi: 10.1016/j.enconman.2023.117304.

[7] A. Marina, S. Spoelstra, H. Zondag, and A. Wemmers, "An estimation of the European industrial heat pump market potential," *Renew. Sustain. Energy Rev.*, vol. 139, Art. no. 110545, 2021, doi: 10.1016/j.rser.2020.110545.

[8] M. U. Ahrens, S. S. Foslie, O. M. Moen, M. Bantle, and T. M. Eikevik, "Integrated high-temperature heat pumps and thermal storage tanks for combined heating and cooling in the industry," *Appl. Therm. Eng.*, vol. 189, Art. no. 116731, 2021, doi: 10.1016/j.applthermaleng.2021.116731.

[9] International Energy Agency, *Net Zero by 2050: A Roadmap for the Global Energy Sector*. Paris, France: IEA, 2021. [Online]. Available: https://www.iea.org/reports/net-zero-by-2050

[10] X. Ma, Y. Du, B. Lei, and Y. Wu, "Energy, exergy, economic, and environmental analysis of a high-temperature heat pump steam system," *Int. J. Refrig.*, vol. 160, pp. 423–436, 2024, doi: 10.1016/j.ijrefrig.2024.01.020.
[11] M. Ramirez, F. Trebilcock-Kelly, J. L. Corrales-Ciganda, J. Payá, and A. H. Hassan, "Experimental and numerical investigation of a novel high-temperature heat pump for sensible and latent heat delivery," *Appl. Therm. Eng.*, vol. 247, Art. no. 122961, 2024, doi: 10.1016/j.applthermaleng.2024.122961.
[12] E. Bellos, D. Gonidaki, A. Nazos, and J. K. Kaldellis, "Feasibility analysis of industrial high-temperature heat pumps in Greece," *Appl. Sci.*, vol. 15, no. 9, Art. no. 5171, 2025, doi: 10.3390/app15095171.
[13] K. M. Adamson *et al*., "High-temperature and transcritical heat pump cycles and advancements: A review," *Renew. Sustain. Energy Rev.*, vol. 167, Art. no. 112798, 2022, doi: 10.1016/j.rser.2022.112798.
[14] X. Hu, Y. Liu, S. Dong, G. Li, Z. Sun, and Y. Liu, "Comparison study of conventional and advanced exergy analysis on cascade high-temperature heat pump system based on experiment," *Case Stud. Therm. Eng.*, vol. 40, Art. no. 102552, 2022, doi: 10.1016/j.csite.2022.102552.
[15] J. Wu, S. Sun, Q. Song, D. Sun, D. Wang, and J. Li, "Energy, exergy, exergoeconomic and environmental (4E) analysis of cascade heat pump, recuperative heat pump and carbon dioxide heat pump with different temperature lifts," *Renew. Energy*, vol. 207, pp. 407–421, 2023, doi: 10.1016/j.renene.2023.03.028.
[16] X. Hu, C. Shi, Y. Liu, X. Fu, T. Ma, and M. Jin, "Advanced exergy and exergoeconomic analysis of cascade high-temperature heat pump system for recovery of low-temperature waste heat," *Energies*, vol. 17, no. 5, Art. no. 1027, 2024, doi: 10.3390/en17051027.
[17] Y. Dong and R. Wang, "When and how to use cascade high-temperature heat pump—its multi-criteria evaluation," *Energy Convers. Manage.*, vol. 309, Art. no. 118435, 2024, doi: 10.1016/j.enconman.2024.118435.
[18] W. Wagner *et al*., "The IAPWS industrial formulation 1997 for the thermodynamic properties of water and steam," *J. Eng. Gas Turbines Power*, vol. 122, no. 1, pp. 150–184, 2000, doi: 10.1115/1.483186.
[19] I. H. Bell, J. Wronski, S. Quoilin, and V. Lemort, "Pure and pseudo-pure fluid thermophysical property evaluation and the open-source thermophysical property library CoolProp," *Ind. Eng. Chem. Res.*, vol. 53, no. 6, pp. 2498–2508, 2014, doi: 10.1021/ie4033999.
[20] R. Span and W. Wagner, "A new equation of state for carbon dioxide covering the fluid region from the triple-point temperature to 1100 K at pressures up to 800 MPa," *J. Phys. Chem. Ref. Data*, vol. 25, no. 6, pp. 1509–1596, 1996, doi: 10.1063/1.555991.
[21] R. Tillner-Roth and H. D. Baehr, "An international standard formulation for the thermodynamic properties of 1,1,1,2-tetrafluoroethane (HFC-134a) for temperatures from 170 K to 455 K and pressures up to 70 MPa," *J. Phys. Chem. Ref. Data*, vol. 23, no. 5, pp. 657–729, 1994, doi: 10.1063/1.555958.
[22] M. E. Mondéjar, M. O. McLinden, and E. W. Lemmon, "Thermodynamic properties of trans-1-chloro-3,3,3-trifluoropropene (R1233zd(E)): Vapor pressure, (p, ρ, T) behavior, and speed of sound measurements, and equation of state," *J. Chem. Eng. Data*, vol. 60, no. 8, pp. 2477–2489, 2015, doi: 10.1021/acs.jced.5b00348.
[23] M. O. McLinden and R. Akasaka, "Thermodynamic properties of cis-1,1,1,4,4,4-hexafluorobutene [R-1336mzz(Z)]: Vapor pressure, (p, ρ, T) behavior, and speed of sound measurements and equation of state," *J. Chem. Eng. Data*, vol. 65, no. 9, pp. 4201–4214, 2020, doi: 10.1021/acs.jced.9b01198.
[24] T. J. Kotas, *The Exergy Method of Thermal Plant Analysis*. London, U.K.: Butterworths, 1985.
[25] B. Zühlsdorf, J. K. Jensen, S. Cignitti, C. Madsen, and B. Elmegaard, "Analysis of temperature glide matching of heat pumps with zeotropic working fluid mixtures for different temperature glides," *Energy*, vol. 153, pp. 650–660, 2018, doi: 10.1016/j.energy.2018.04.048.
[26] M. Gambini, M. Manno, and M. Vellini, "Energy and exergy analysis of transcritical CO2 cycles for heat pump applications," *Sustainability*, vol. 16, no. 17, Art. no. 7511, 2024, doi: 10.3390/su16177511.
[27] L. Kong *et al*., "Transcritical–transcritical cascade CO2 heat pump cycles for high-temperature heating: A numerical evaluation," *Appl. Therm. Eng.*, vol. 238, Art. no. 122005, 2024, doi: 10.1016/j.applthermaleng.2023.122005.
[28] E. Vieren, T. Demeester, W. Beyne, A. Arteconi, M. De Paepe, and S. Lecompte, "The thermodynamic potential of high-temperature transcritical heat pump cycles for industrial processes with large temperature glides," *Appl. Therm. Eng.*, vol. 234, Art. no. 121197, 2023, doi: 10.1016/j.applthermaleng.2023.121197.
[29] S. Koochakinia, A. Ebrahimi-Moghadam, and M. Deymi-Dashtebayaz, "Techno-environmental analyses and optimization of a utility boiler based on real data," *Sustainability*, vol. 14, no. 5, Art. no. 2592, 2022, doi: 10.3390/su14052592.
[30] Y. Huang, G. Li, X. Tang, K. Huang, W. Zhao, and J. Zhang, "Thermodynamic analysis of a modified cascade high-temperature heat pump with zeotropic mixtures for heating production up to 200 °C," *Energy Convers. Manage.*, vol. 324, Art. no. 119307, 2025, doi: 10.1016/j.enconman.2025.119307.
[31] J. Spale, A. J. Hoess, I. H. Bell, and D. Ziviani, "Exploratory study on low-GWP working fluid mixtures for industrial high-temperature heat pump with 200 °C supply temperature," *Energy*, vol. 308, Art. no. 132677, 2024, doi: 10.1016/j.energy.2024.132677.
[32] J. Feng, J. Gao, B. Hu, R. Wang, and Z. Xu, "A mass-coupled hybrid absorption–compression heat pump with output temperature of 200 °C," *Energy*, vol. 312, Art. no. 133608, 2024, doi: 10.1016/j.energy.2024.133608.